An Energy Tranfer Study of the Interface Thickness in Blends of Poly(butyl methacrylate) and Poly(2-ethylhexyl methacrylate)

J. P. S. Farinha,† O. Vorobyova, and M. A. Winnik*

Department of Chemistry, University of Toronto, 80 St. George Street, Toronto, Ontario, Canada M5S 3H6

Received January 20, 2000; Revised Manuscript Received May 16, 2000

ABSTRACT: We propose a model to describe energy transfer between donors and acceptors chemically attached to the two different components of a polymer blend. The model describes the case of one polymer dispersed as spheres of identical diameter in a continuous matrix of the second polymer. The model takes explicit account of the segment distribution of the two polymers in the interface region. We used this model to characterize the interface between poly(butyl methacrylate) (PBMA) and poly(2-ethylhexyl methacrylate) (PEHMA) domains in a binary blend. The blend was prepared by casting films onto a solid substrate from mixed aqueous latex dispersions of the two polymers. The dispersions were prepared by emulsion polymerization under conditions in which both components were formed as spherical particles with a very narrow size distribution. By using a 14:1 particle ratio of PEHMA to PBMA, we obtained films in which the 120 nm PBMA particles were surrounded by the PEHMA matrix. For the ion-exchanged latex blend, the interface thickness in the film freshly prepared at room temperature was $\delta = 21 \pm 2$ nm and upon annealing broadened to $\delta = 25 \pm 2$ nm. Because of the low degrees of polymerization for the samples, it is difficult to have confidence in the value of the Flory−Huggins parameter χ calculated from the experimental value of δ, because the correction for the finite length of the component is larger than the term that depends on the interface width. Keeping in mind the limitations of this calculation, we estimate that χ is approximately equal to 0.02−0.03.

Introduction

Polymer blends have been studied for many years.[1] While a small fraction of polymer mixtures are fully miscible at the molecular level, most polymer blends are not.[2] One often refers to polymer blends as "immiscible" if the blend exhibits two glass transition temperatures identical to those of the individual components. Many polymer blends are not completely immiscible; some segment interpenetration occurs at the interface between the individual domains. In these systems, the volume fraction of the interfacial region may be too small to detect by differential scanning calorimetry (DSC) or by dynamic mechanical analysis (DMA). Other techniques, however, such as the nonradiative energy transfer method pioneered for the study of polymer blends by Morawetz and co-workers,[3] show that these polymer blends are best described as having limited miscibility. The theory of polymer blends describes the breadth of the interface separating the two materials in terms of the Flory−Huggins parameter χ, which describes the free energy of interaction between segments of the two polymers.[4,5]

One of the attractive features of polymer blends as materials is that the presence of separate domains with different compositions can lead to synergistic interactions and material properties that are enhanced compared to those of the individual components. All impact-modified plastics, for example, take advantage of this synergy. Another attraction is that blends can be prepared by mixing traditional polymers. These polymers are much less costly than polymers prepared from new specialty monomers.

Of all the properties of phase-separated polymer blends, the interface between adjacent phases is the least understood. Polymer interfaces ("interphases") are known to be much thicker than interfaces in inorganic materials; nevertheless, they still represent a small fraction of the total volume of the material. The limited amount of information available about polymer−polymer interfaces is a direct consequence of the fact that there are few techniques that allow one to study these interfaces directly. The most powerful method for studying polymer−polymer interfaces is specular neutron reflectivity.[6] In this technique, one prepares a thin sandwich from thin films of two different polymers, one of which is deuterated to provide contrast. The sample is annealed to bring the system to equilibrium. Segmental diffusion at the interface leads to a gradient in contrast at the interface between the two components. The angular dependence of the reflected signal is rich in information. The major shortcoming of this and all scattering techniques is the difficulty in distinguishing between a segment-density distribution at the interface and waviness of the interface. Only the former contributes to the "thickness" of the interface.[7]

Small-angle X-ray scattering (SAXS) and small-angle neutron scattering (SANS) are also able in principle to provide information about interface thickness.[8] One can carry out scattering experiments on a variety of different blend morphologies, including the case of droplets of one component dispersed in a matrix of a second component. Information about the interface in these experiments is obtained in a somewhat more indirect manner. One analyzes the scattering function (angular dependence of the scattering intensity) by comparing the data to that expected for a similar system with sharp interfaces between the domains. One introduces the concept of a finite interface thickness into the model to bring the model scattering function into concordance with the experimental data.

† On leave from: Centro de Química-Física Molecular, Instituto Superior Técnico, Av. Rovisco Pais, 1049-001 Lisbon, Portugal. E-mail: farinha@ist.utl.pt.

* To whom correspondence should be addressed. E-mail: mwinnik@chem.utoronto.ca.

10.1021/ma0000935 CCC: $19.00
Published on Web 07/15/2000

In this paper, we examine the possibility that direct nonradiative energy transfer (DET) experiments will allow one to determine the thickness of the interface between adjacent phases in polymer blends. In a DET experiment, one examines the rate and efficiency of energy transfer between two different dyes in the system: a donor dye, which is excited selectively, and an acceptor dye, which accepts energy from the excited donor.[9] We derive equations to show that this type of information is in principle available if the minor phase is present as a dispersion of droplets all of the same size. We test this idea by examining a blend of two acrylate polymers: a dispersion of poly(butyl methacrylate) (PBMA) droplets in a poly(2-ethylhexyl methacrylate) (PEHMA) matrix. The PBMA particles have a glass transition temperature (T_g) near room temperature. The PEHMA particles have a much lower T_g, about −10 °C. The blends we examine have as the minor component a dispersion of PBMA nanospheres in a matrix of PEHMA.

To our knowledge, there are as yet no experiments that provide quantitative information about the thickness of the interface between two acrylate polymers. Indirect information about the interface between PEHMA and poly(methyl methacrylate) (PMMA) was reported by Cameron et al.[10] based upon electron paramagnetic resonance (EPR) measurements involving polymers containing a covalently bound nitroxide as a spin-label. These authors were interested in the location of the chain ends in binary polymer blends. To investigate this issue, the authors used group transfer polymerization to prepare samples in which the nitroxide was attached to an end of one of the polymers, either the PEHMA or the PMMA. The polymers prepared in this way had relatively narrow molar mass distributions.

Blends were prepared by freeze-drying a mixture of the two polymers in dilute solution in benzene. The samples were subsequently annealed. Traditional measurements such as scanning calorimetry and dynamic mechanical measurements suggested that the polymers are essentially immiscible, and by phase contrast optical microscopy, separate domains of micrometer dimensions could be seen. The striking feature of the EPR results in these hard−soft polymer blends is that the unlabeled component in the blend has a marked effect on the mobility of a nitroxide label attached to the end of the other polymer. For example, when the end of the PMMA was labeled, it exhibited little mobility in the glassy environment of pure PMMA itself ($T_g \approx 100$ °C). In PMMA blends with the much softer PEHMA, the spin-label at the ends of the PMMA chain showed a mobile component in the EPR spectrum, a sign that the chain ends were located in an interfacial region with higher mobility. A similar conclusion could be drawn from experiments in which the PEHMA ends contained the nitroxide label. These labels in PEHMA itself were in a mobile environment, whereas in blends with unlabeled PMMA, the mobility of some of the chain ends was strongly reduced.

Cameron et al. carried out similar experiments with polymers labeled at random along the backbone. Here the effect was much less prominent. The authors concluded first that the EPR experiments indicated partial miscibility for the two polymers. They also concluded that their experiments showed that the chain ends were enriched in the polymer−polymer interface, in accord with a theoretical prediction of Helfand and co-workers.[4,11] These results suggested to the authors that the interface between the PMMA and PEHMA domains in these blends is diffuse and relatively thick. One would have a much better understanding of this type of blend if one could measure the thickness of the interface directly.

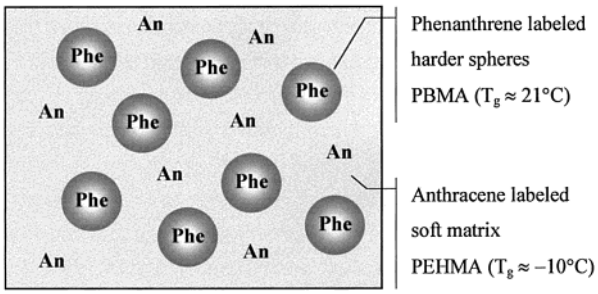

Figure 1. A drawing showing the expected morphology of a latex blend film containing PBMA nanospheres dispersed in a PEHMA matrix.

In this paper, we describe experiments that allow us to determine the interface thickness in a polyacrylate blend. We use DET experiments on dye-labeled polymers and employ the same Helfand−Tagami theory[4] cited above to interpret the results. In these experiments, we examine a somewhat different blend of acrylate polymers than that described by Cameron et al. Our choice was based on a search for a model system, as part of an ongoing project, that we could use to study droplet coalescence in polymer blends under shear. For these experiments, we needed a low-T_g matrix phase, for which PEHMA is an excellent choice. For the dispersed phase we needed a polymer with a lower T_g than PMMA, so that droplet encounters at temperatures below 100 °C would lead to coalescence. Thus, we chose PBMA to serve this role.

Our approach requires a system in which all of the polymer in the dispersed phase is present as spheres of the same diameter. To ensure that all of the PBMA droplets are the same size, we prepared these particles by emulsion polymerization. We used a fluorescent comonomer, 9-vinylphenanthrene, to introduce covalently bound donor dyes (1 mol %) into the PBMA phase. The particles obtained have a very narrow size distribution, but the polymers in the particles have a rather broad molecular weight distribution. Since the particles are spherical with a diameter of ca. 120 nm, we refer to these as "nanospheres". We also prepared the PEHMA component by emulsion copolymerization, using 9-anthryl methacrylate to obtain particles with covalently bound acceptor dyes (1 mol %). In this case, the choice of emulsion polymerization for the PEHMA component was simply one of convenience: it allowed us to formulate an efficient blend preparation procedure. The two aqueous dispersions could be mixed and cast as a film on a solid support. As the water evaporates, a dense film is formed. The soft PEHMA particles become deformed during the drying process into cells with the shape of Voronoi polyhedra.[12] Upon standing, all traces of the initial cellular morphology of the PEHMA phase are lost through polymer diffusion across the boundary between PEHMA cells. As we show below, the PBMA nanospheres, which represent about 10 vol % of the blend, form the dispersed phase. In Figure 1 we present a cartoon of the morphology we expected for these blends.

We carry out donor fluorescence decay measurements of direct nonradiative energy transfer in the blends

Table 1. Latex Characteristics

	fluorescent dye	diameter (nm)	$10^{-3}M_w$[a]	$10^{-3}M_n$[a]
PBMA-Phe	phenanthrene	119	35.7	16.7
PBMA-An	anthracene	119	33.9	18.3
PEHMA-An	anthracene	97	56	27
PEHMA		99	140	48

[a] Determined using PMMA as a standard in size exclusion chromatography measurements. This analysis ignores a nonfluorescent peak at higher M due to the seed particle.

prepared as described above. We interpret the shape of these decay profiles in terms of a model in which the thickness of the interface between the PBMA and the PEHMA components is the fitting parameter. This model we develop represents a special case of the more general model describing direct energy transfer in systems of restricted geometry in which the distribution of donor and acceptor dyes is characterized by spherical symmetry.[13−16] This model takes into account the size and shape of the domains in which the dyes are distributed and the variation in their concentration over the domains. To proceed with the analysis, one must introduce a function describing the radial variation of the dye concentration. In this case, for the shape of the distributions of the two blend components across the interface, we employ the hyperbolic tangent function derived by Helfand and Tagami (HT) for interfaces in strongly segregated polymers.[11] Because the HT model was derived for planar structures, we modify this model to account for the curvature of the interface at the surface of spherical particles.

The paper is organized as follows: We begin with a brief Experimental Section. We then present the models that serve as the basis for this paper, the structural (H−T) model for the distribution of junctions across the polymer−polymer interface, and the model employed for describing energy transfer kinetics. Included in this section is a description of the simulation of fluorescence decay curves using the DET distribution model. The Results and Discussion section begins with an analysis of the morphology of the blends we prepared. This is followed by an analysis of the fluorescence data using the DET distribution model. We end with our conclusions.

Experimental Section

Latex Synthesis. Poly(2-ethylhexyl methacrylate) (PEHMA) and poly(butyl methacrylate) (PBMA) latex dispersions were prepared by two-stage seeded emulsion polymerization, with the fluorescent dye introduced during the second stage. The details of the synthesis are described elsewhere. Anthracene-labeled PEHMA latex and nonlabeled PEHMA latex were prepared by Pham.[17] Both anthracene- and phenanthrene-labeled PBMA were synthesized by Feng.[18] The size and molecular weight of all latex used in this study are listed in Table 1.

Molecular weights of PBMA and PEHMA polymers were determined by size exclusion chromatography, first with a column calibrated with PMMA standards and later with a triple detection system, consisting of refractive index (RI), light scattering, and viscosity detectors. Using the RI and PMMA standards, we find for PBMA $M_w = 35\,000$ and $M_n = 17\,000$. For PEHMA, we obtain $M_w = 56\,000$ and $M_n = 27\,000$. With the triple detector, we obtained $M_w = 210\,000$ and $M_n = 31\,000$ for PBMA, indicating a small amount of a high molar mass component not detected by the RI detector alone. No meaningful signal for PEHMA was obtained with the triple detector. The material of highest molar mass is formed during the synthesis of the seed particles, which is carried out in the absence of any chain transfer agent. The seed polymer also contains no fluorescent dye. The seed represents 8 wt % of the final particles.

Sample Preparation. Known amounts of PEHMA and PBMA dispersions were mixed to give a blend composition of 90% PEHMA and 10% PBMA by weight. The mixture (8 mL) was degassed and cast on freshly cleaved mica sheet (8 × 8 cm) and then left overnight to dry uncovered at ambient conditions (temperature 23−25 °C, relative humidity 50−60%). These films dried from the edges inward. Most of the films became clear in about 6 h, but additional time was necessary for the turbid spot in the center of the film to become clear. It was estimated that the total drying time was about 8−10 h. The dry films were clear with a thickness of about 400−500 μm. The long drying time was a consequence of the thickness of the films, which were subsequently used in rheology experiments.

In some experiments, before casting, the latex mixture was diluted to yield a 5 wt % dispersion and treated with an ion-exchange resin (Bio-Rad mixed-bed resin AG 501-X8) to remove surfactant SDS (sodium dodecyl sulfate) and other low molecular weight inorganic compounds used in the latex synthesis. In that case, the mixture was stirred twice for 2 h with a fresh portion of the resin, added in the amount of 20 wt % of the total latex solids. The resin beads were then removed by filtration, and the film preparation was continued as described above. The dry films were clear with a uniform thickness of ca. 200 μm.

Laser Scanning Confocal Fluorescence Microscopy (LSCFM). A Zeiss LSM 510 confocal instrument with a water immersion C-Apochromat 63x/1.2w corrected objective was used. Anthracene was excited with the 364 nm band of a coherent Enterprise ENTC-635 laser. A 385 nm cutoff filter was used to prevent excitation light from coming to the detector. The confocal pinhole was set at 79 μm, which corresponds to an optical slice thickness of 0.6 μm.

Atomic Force Microscopy (AFM). AFM images of latex films surfaces were obtained with Nanoscope III (Digital Instruments, Santa Barbara, CA) using silicone nitride tips. The images were obtained in the contact mode.

Fluorescence Measurements. Steady-state fluorescence measurements were carried out with a SPEX Fluorolog 212 fluorescence spectrometer. Fluorescence decay measurements were obtained by the single-photon timing technique.[19] Excitation with a deuterium-filled coaxial flash lamp gives nanosecond time resolution. Phenanthrene was excited at 300 nm, and the emission was collected at 348 nm, using a cutoff filter in front of the detector in order to decrease the amount of scattered light in the signal. The instrumental response function was obtained by the mimic lamp method,[20] from the decay of a solution of *p*-terphenyl in aerated cyclohexane (τ = 0.96 ns). A correction for the scattered light contamination of the decays was carried out as described by Martinho et al.[21]

The Model: Energy Transfer across a Polymer Interface

Our long-term objective is to develop the means to use DET experiments to characterize polymer blends at the level of the interface between the two polymer components, given the sizes and shapes of the different domains in the blend. As a step in this direction, we consider the case of a binary blend with the minor component present as spheres of identical size. In this section we describe the model for energy transfer between two dyes attached to two components in a binary polymer blend. The dyes are assumed to be attached at random to their respective polymers. Thus, the spatial distribution of dyes follows the segment distribution of the individual polymers. We imagine that the polymer containing the donor dye is present as a spherical droplet surrounded by a matrix of the acceptor-labeled polymer. Since the model is based upon a single droplet in a continuous matrix, the model corresponds to a

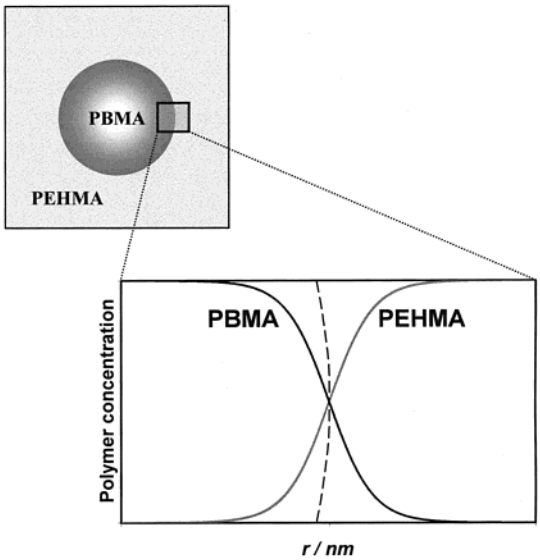

Figure 2. A drawing of the polymer segment density profile across the interface between a PBMA microsphere and the surrounding PEHMA matrix.

system in which all of the dispersed droplets are identical in size. Thus, all droplets are related by translational symmetry.

The model has two parts. First, one needs a structural model to describe the distribution of polymer segments in the region of the polymer interface. In addition, one needs a kinetic model to describe the rate of direct nonradiative energy transfer in the restricted geometry of the interfacial domain.

Structure of the Polymer Interface. To begin, we need a model able to describe the concentration profile of the blend components as a function of the parameters that control the extent of mixing between the polymers at the interface. A useful starting point is to assume that the general shape of the polymer segment distribution can be described by a hyperbolic tangent function, in accord with the theory derived by Helfand and Tagami for polymer blends with planar interfaces. We modify the distribution obtained from the HT model in order to account for the spherical geometry of the interface in our system. Our approach is similar to that described in ref 16 for the case of spherical block copolymer micelles with donor and acceptor groups attached to the junction.

The distributions of the donor dyes (D) in the PBMA nanosphere and the acceptor dyes (A) in the surrounding PEHMA matrix are described by

$$g_D(r) = 0.5\{1 - \tanh[2(r - R_s)/\delta]\} \quad (1a)$$

$$g_A(r) = 0.5\{1 + \tanh[2(r - R_s)/\delta]\} \quad (1b)$$

where δ is a measure of the interface thickness and R_s the radius of the PBMA particle. The interface thickness δ is related to the Flory−Huggins χ parameter between the polymers

$$\delta = \frac{2b}{\sqrt{6\chi}} \quad (2)$$

where b is the statistical segment length. The shape of the distributions is presented in Figure 2.

In Figure 3 we present the donor and acceptor distribution functions calculated for a particle of radius

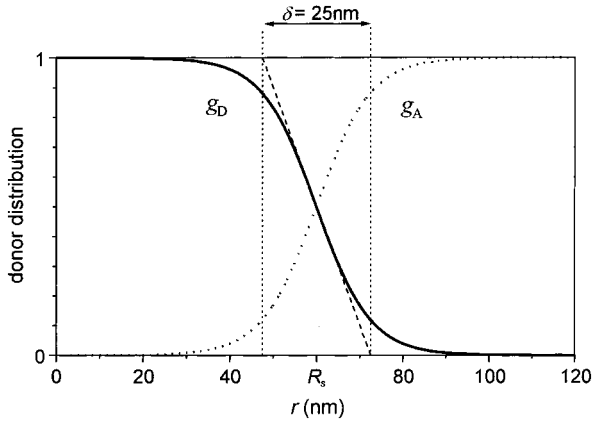

Figure 3. Distribution functions of donor and acceptor in a blend of 10 wt % phenanthrene-labeled PBMA spheres and 90 wt % anthracene-labeled PEHMA, calculated for a particle of radius $R_s = 60$ nm and an interface thickness $\delta = 25$ nm. The interface thickness parameter δ is obtained from the tangent to the distribution function at the position of the initial particle surface, R_s.

$R_s = 60$ nm and interface thickness $\delta = 25$ nm. The definition of the interface thickness parameter δ is depicted in Figure 3. It is obtained from the tangent to the distribution function at the position of the initial particle surface R_s.

Energy Transfer Kinetics. For a dipole−dipole coupling mechanism, Förster[22,23] showed that the rate of energy transfer $w(r)$ between a donor and an acceptor depends on their separation distance r

$$w(r) = \frac{\alpha}{r^6} \quad (3a)$$

$$\alpha = \frac{3R_0^6\kappa^2}{2\tau_D} \quad (3b)$$

where τ_D is the donor fluorescence lifetime in polymer films labeled with donor only; R_0 is the critical Förster distance, with $R_0 = 2.3 \pm 0.1$ nm for the present system.[24] The term κ^2 is a dimensionless parameter related to the relative orientation of the donor and acceptor transition dipole moments.[25,26]

According to eq 4, if the donors and acceptors are homogeneously distributed in an infinite volume, with a constant separation r between each pair, the donor decay function is still exponential but decays more rapidly than the decay function for the unquenched donor

$$I_D(t) = \exp\left(-\frac{t}{\tau_D}\right)\exp[-w(r)t] \quad (4)$$

On the other hand, for energy transfer to a random distribution of acceptors in a three-dimensional Euclidean space, the donor decay function will have the stretched exponential form first derived by Förster.[22,23]

$$I_D(t) = \exp\left(-\frac{t}{\tau_D}\right)\exp\left[-P\left(\frac{t}{\tau_D}\right)^{0.5}\right] \quad (5)$$

The parameter P depends on the local concentration of acceptors and on the averaged relative orientation κ^2 of the donor and acceptor transition moments

$$P = c_\Delta \left(\frac{3\kappa^2}{2}\right)^{0.5} \Gamma(0.5) \tag{6}$$

where c_Δ is the number of acceptors in a sphere of radius R_0; Γ is the Gamma function, with $\Gamma(0.5) = \pi^{0.5}$.

Quantum Efficiency of Energy Transfer. The quantum efficiency of energy transfer Φ_{ET} is defined as

$$\Phi_{ET} = 1 - \frac{\int_t I_D(t)\, dt}{\int_t I_D^0(t)\, dt} = 1 - \frac{A}{A_0} \tag{7}$$

where $I_D(t)$ is the fluorescence decay of a film labeled with donor and acceptor, $I_D^0(t)$ is the decay of a film labeled only with donor, and A and A_0 are the integrals that correspond to the areas under the decay curves. The integral of $I_D^0(t)$ is simply equal to the unquenched donor lifetime $A_0 = \tau_D$. One of the ways to evaluate the integral in eq 7 from the experimental data is to fit the decay curves to a suitable equation first and then to integrate the equation analytically using the fitting parameters obtained.

The Förster model, eq 5, is strictly applicable only to homogeneous distributions of donors and acceptors in a volume that can be considered infinite when compared to R_0. In the system under consideration here, the donors and acceptors are confined to a volume which is small enough to be sensitive to finite size effects, and their distribution is not uniform. In our previous attempts to study these systems, we have used eq 8 as a phenomenological expression to approximate the extent of mixing in latex films labeled with donor and acceptor dyes[24]

$$I_D(t) = a_1 \exp\left(-\frac{t}{\tau_D}\right) + a_2 \exp\left(-\frac{t}{\tau_D}\right) \exp\left[-\beta\left(\frac{t}{\tau_D}\right)^{0.5}\right] \tag{8}$$

Here we use eq 8 as a mathematical function to fit individual donor fluorescence decay profiles. We ascribe no physical meaning to the fitting parameters a_1, a_2, and β in eq 8. Instead, we use these parameters to integrate the expression analytically from $t = 0$ to $t = \infty$, to yield the fluorescence intensity that corresponds to the area A under each decay curve

$$A = \int_0^\infty I_D(t)\, dt = \tau_D\left[1 - \left(\frac{a_2}{a_1 + a_2}\right)\sqrt{\pi}\tau_D\left(\frac{\beta}{2}\right) \exp\left(\frac{\beta}{2}\right)^2 \operatorname{erfc}\left(\frac{\beta}{2}\right)\right] \tag{9}$$

Using eqs 7 and 9, the quantum efficiency of energy transfer Φ_{ET} can then be calculated as

$$\Phi_{ET} = \left(\frac{a_2}{a_1 + a_2}\right)\sqrt{\pi}\tau_D\left(\frac{\beta}{2}\right) \exp\left(\frac{\beta}{2}\right)^2 \operatorname{erfc}\left(\frac{\beta}{2}\right) \tag{10}$$

where the parameters a_1, a_2, and β are obtained from the fit of the donor decay to eq 8 for a sample containing donor and acceptor.

The Φ_{ET} values calculated from eq 10 are obtained in a model-free way, with minimal assumptions in the data analysis. This parameter can be used to characterize the extent of miscibility of the components in a polymer blend. As Morawetz and co-workers [3] have shown, if one polymer is labeled with an energy donor and the other with an energy acceptor, an increase in the miscibility of the blend components will bring an increasing number of the donors and acceptor into proximity, increasing Φ_{ET}.

Fitting Fluorescence Decay Profiles in Terms of the HT Model. To examine the possibility that deeper information about the blends can be obtained from the detailed shape of the donor decay profile, we have to relate the Helfand−Tagami description of the polymer segment density distribution across the interface in a polymer blend, eq 1, with the theory of energy transfer in restricted geometry. We assume that the distribution of donors follows the segment distribution of the polymer to which the donor is attached, and that the distribution of acceptors follows the segment distribution of the other polymer in the blend. It is not possible to obtain the segment distribution function itself from the analysis of the fluorescence decay profiles. Instead, we introduce these distribution functions into the process of fitting individual experimental decay profiles. On the basis of the theoretical analysis described below, we simulate fluorescence decay curves for various trial functions in which the interface thickness is treated as the variable parameter. The other parameters describing the system are assumed to be known independently.

Shape of the Fluorescence Decay Profile. In the present system there is a nonhomogeneous spatial distribution of acceptors and donors. As a consequence, the donor fluorescence decay rate depends on both the distribution of acceptors around each donor and the distribution of donors itself. According to the distribution model for energy transfer in spherical systems,[13−16] the donor decay function for a delta-pulse excitation is described by

$$I_D(t) = \exp\left(-\frac{t}{\tau_D}\right)\int_{V_s} C_D(r_D)\, \varphi(t,r_D) r_D^2\, dr_D \tag{11a}$$

$$\varphi(t,r_D) = \exp\left(-\frac{2\pi}{r_D}\int_{R_e}^\infty \{1 - \exp[-w(r)t]\}\left[\int_{|r_D - r|}^{r_D + r} C_A(r_A) r_A\, dr_A\right] r\, dr\right) \tag{11b}$$

where V_s is the volume containing the donors that initially were in a donor labeled particle, τ_D is the unquenched fluorescence lifetime of the excited donor, and $\varphi(t,r_D)$ is the probability of energy transfer of a donor located at r_D. $C_D(r)$ and $C_A(r)$ are the respective concentration profiles of donors and acceptors across the interface, described by eq 1.

The donor concentration profile $C_D(r)$ is described by eq 1 and can have any convenient concentration units, since eq 11a will later be multiplied by a normalization constant. The concentration profile of acceptor is $C_A(r) = C_A^0\, g_A(r)$, with $g_A(r)$ described by eq 1b and C_A^0 the initial average acceptor concentration in the acceptor labeled particles. $C_A(r)$ must have units of number density. The encounter radius, R_e, is the minimum distance between donor and acceptor at which the effect of dipolar energy transfer can still be observed in the donor fluorescence. It is usually set equal to the sum of the donor and acceptor van der Waals radii.[27] However, over a significant range of values, the donor decay functions calculated are not very sensitive to changes in this cutoff parameter.[16]

The numerical evaluation of eq 11 using the distribution functions in eq 1 raises a number of technical points. First, we calculate all the integrals using a

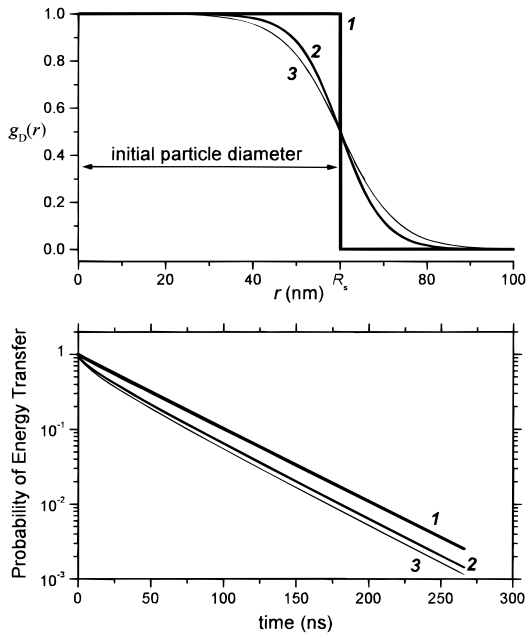

Figure 4. (top) Radial distribution function of the donor-labeled polymer for a particle of radius $R_s = 60$ nm and an interface thickness of $\delta = 0$ nm (1), $\delta = 20$ nm (2), and $\delta = 26$ nm (3). (bottom) Simulated donor decay functions, corresponding to the radial distributions shown above, calculated according to eqs 1 and 11, for a blend containing 90 wt % acceptor-labeled PEHMA and 10 wt % donor-labeled PBMA spheres.

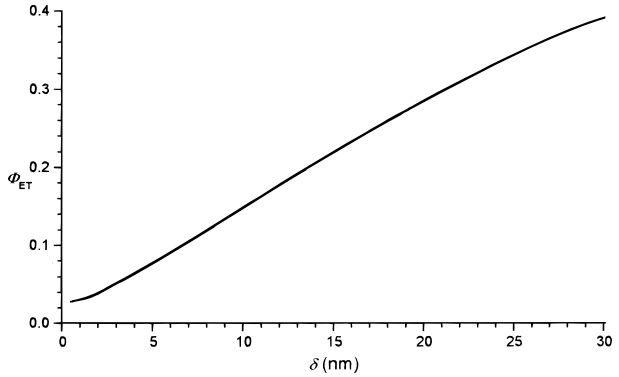

Figure 5. Energy transfer efficiency Φ_{ET} calculated from simulated fluorescence decay curves with different interface thicknesses δ. As the interface becomes thicker, more donors and acceptors are mixed and there is more energy transfer.

simple trapezoidal rule because more sophisticated adaptive quadrature routines are not stable when used in the evaluation of multiple integrals.[28] Second, since $w(r)$ is a very sharply peaked function of r for all accessible experimental times, the integration over r in eq 11b was evaluated only from R_e to $3R_0$. Finally, the donor and acceptor distributions, eq 1, were truncated in order to simplify the numerical calculations. For the present system we truncate the distribution at $R_s \pm 2.5\delta$. This includes almost all of the dyes (Figure 3).[16]

Simulation Procedure. The system we simulated consists of a donor-labeled sphere in a continuous acceptor labeled matrix, with an interface of variable width. To evaluate the extent of mixing at the interface in real samples, we compare the experimental data (energy transfer quantum yields, donor decay profiles) with simulations of these results. In this way we can examine the effect of the thickness of the interface between the particles and the matrix on energy transfer between the donor and acceptor dyes attached to the blend components.

We began by simulating a series of donor fluorescence decay functions calculated according to eqs 1 and 11, with the interface ranging in thickness from 0 to 30 nm. We chose input parameters characteristics of the blend of interest, a blend consisting of 10 vol % phenanthrene-labeled PBMA, present as isolated spheres of identical diameter, surrounded by the continuous anthracene-labeled PEHMA matrix. We used $\kappa^2 = 0.478$, $R_0 = 2.3$ nm, $\tau_D = 45.5$ ns, and a cutoff distance $R_e = 0.5$ nm. The donor-labeled sphere has a radius $R_s = 60$ nm, and the average concentration of the acceptor in the matrix is $C_A^0 = 0.05$ M. In Figure 4 we plot some of the simulated donor survival probability curves, for interface thickness $\delta = 0$ nm, $\delta = 20$ nm, and $\delta = 26$ nm. These curve represent "noise-free" data obtained directly from the simulations. The calculated donor distribution profiles corresponding to these curves are also shown.

From Figure 4 we see that broader interfaces lead to faster donor decay rates and steeper donor decay profiles, particularly at early times. As the interface becomes thicker, more donors and acceptors are in proximity. As a consequence, both the rate and the efficiency of energy transfer increase. The Φ_{ET} data in Figure 5 were calculated by integrating the simulated decay profiles using eq 10. The relation between Φ_{ET} and δ is not linear. The value of the energy transfer efficiency calculated for $\delta = 0$ nm represents the amount of energy transfer taking place across a perfectly sharp interface. For this system comprised of 120 nm diameter donor labeled spheres and 1 mol % acceptor in the surrounding matrix, $\Phi_{ET}(\delta=0) = 0.03$.

Results and Discussion

The blends we describe are obtained by drying aqueous dispersions consisting of 90 wt % of anthracene-labeled PEHMA particles, with a diameter $d = 100$ nm, and 10 wt % of phenanthrene-labeled PBMA particles ($d = 120$ nm), each with a narrow size distribution. We will refer to this blend as a 9:1 blend of PEHMA and PBMA. Assuming that the polymers have similar densities, the ratio of donor- to acceptor-labeled particles is 1:14. Therefore, the donor-labeled PBMA particles are considered to be imbedded in the softer acceptor-labeled PEHMA continuous matrix, as depicted in the cartoon in Figure 1.

In the bulk state, the PEHMA sample has a T_g of approximately −10 °C, and the low molecular weight PBMA sample used here has $T_g = 21$ °C.[29] Due to the low glass transition temperatures of the components, we expect that some polymer diffusion will take place during sample preparation. Feng et al.[29] have studied the diffusion of PEHMA in latex films at room temperature. On the basis of these results, we expect that diffusion within the PEHMA phase will convert the initial cellular structure of the latex film into a uniform matrix. We also expect that some segmental diffusion will take place at the PEHMA−PBMA interface during sample preparation, leading to mixing of the segments of the two components. This is a hypothesis that we have tested in the course of the experiments to be described below.

Polymer Domains in the Blend. When we designed these experiments, we assumed that an aqueous latex dispersion containing a relatively small amount of a second component would be randomly mixed if the two components were of similar size and had similar stabi-

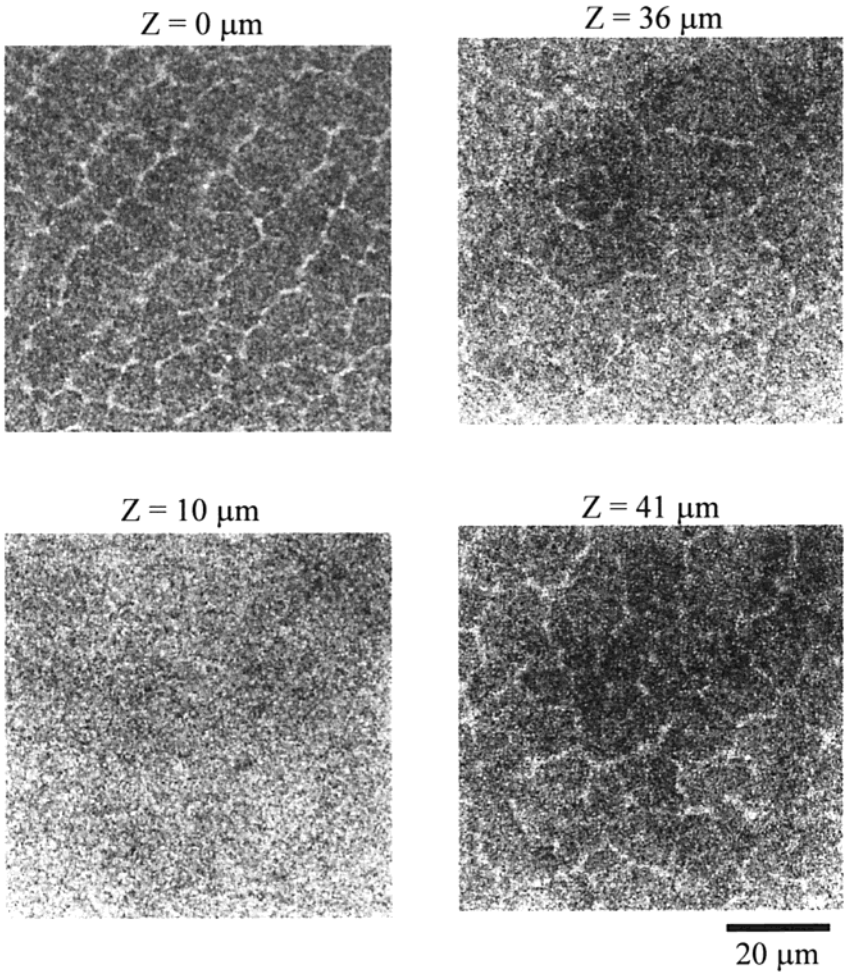

Figure 6. LSCFM images taken at different depths of a film cast from a mixture of 90 wt % unlabeled PEHMA and 10 wt % anthracene-labeled PBMA, containing about 2 wt % of SDS surfactant. Individual particles cannot be imaged because the size of the latex particles is below the resolution limit of the instrument, but aggregates of a few particles would be detected. Some exclusion of the PBMA is observed at the air−polymer surface and in some of the sections imaged inside the film. From other sections just below the film surface (10−25 μm) we collect uniform fluorescence signals.

lizing groups at their surface. Since the distribution of the minor component in the film formed as the dispersion dries must reflect the distribution of particles in the aqueous phase at high solids, we assumed that there would be little driving force for aggregation of the PBMA nanospheres in the blend. We imagined that these polymer films could be described by a morphology in which PBMA "hard" spheres are imbedded at random in the softer PEHMA matrix as shown in Figure 1.

To examine the morphology of the film, we carried out atomic force microscopy (AFM) and laser scanning confocal fluorescence microscopy (LSCFM) measurements on these films. We performed LSCFM measurements on 400−500 μm thick films cast from 9:1 mixtures of unlabeled PEHMA and anthracene-labeled PBMA (Figure 6). Only the fluorescence from the anthracene groups attached to the PBMA can be imaged. No signal is detected from the PEHMA matrix. Since the size of the latex particles is below the resolution limit of the instrument, individual particles cannot be imaged, but aggregates of a few particles would be readily detected. In films prepared from dispersions ion-exchanged to remove the surfactant SDS, we collect a uniform fluorescence signal that indicates that the PBMA particles are homogeneously distributed in the PEHMA matrix.

For films containing about 2 wt % of SDS surfactant, we observe some local phase separation of the two polymers (Figure 6, sections at depths of 0 and 41 μm) throughout the film with the exception of the region just under the film surface at the air interface. In this region we observe a uniform fluorescence signal (e.g., the section at 10 μm from the film surface, Figure 6), indicating the presence of labeled PBMA but the absence of aggregates. After annealing this film at 100 °C for 1 h, we observed no apparent change in morphology of the film by LSCFM. The aggregation seen in other regions of the film was unexpected and seems to reflect the formation of flocs in the aqueous phase during sample preparation. This phenomenon is rather complex. The aggregates seen in Figure 6 are formed when we mix concentrated dispersions (ca. 30 wt %) of the two particles, but these aggregates do not appear in the film when the mixed dispersion is diluted to 5 wt % prior to casting a film. Under these circumstances, we do, however, see some aggregates at the very edge of the film. We are investigating this effect and will defer further comments to a future publication.[30]

To determine whether the aggregation seen on the micrometer scale in Figure 6 affects the particle distribution on the nanometer scale, we obtained AFM images of the surface of a film cast from a 9:1 mixture of PEHMA and PBMA (not ion-exchanged, 2 wt % SDS present) onto a mica plate (Figure 7). In this image, we observe individual spheres at the surface, embedded

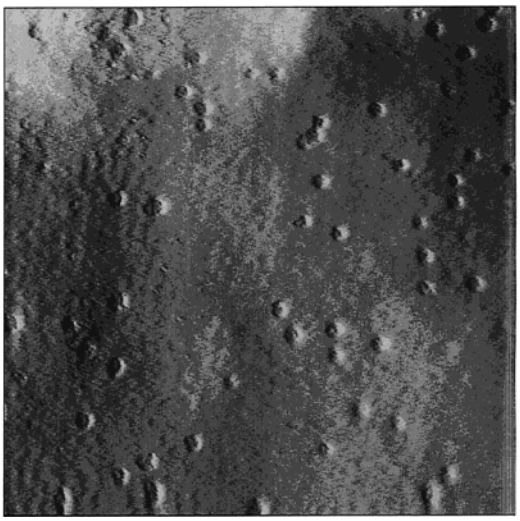

Figure 7. An AFM image of the polymer/air surface of a film cast from a mixture of 90 wt % PEHMA and 10 wt % PBMA containing SDS surfactant. The image is 5 μm by 5 μm. Individual PBMA spheres embedded in the PEHMA matrix can be identified.

Table 2. Energy Transfer Efficiencies in PBMA/PEHMA Binary Blends

	Φ_{ET}	
	with 2 wt % of SDS	without SDS
newly formed film (4 °C)	0.25	
newly formed film (20 °C)	0.29	0.25
annealed 1 h at 60 °C	0.33	0.33
annealed 1 h at 90 °C	0.33	

in a continuous matrix. The spheres in this image have a measured average diameter of about 150 nm, which corresponds to the diameter of the PBMA particles (120 nm) determined by dynamic light scattering, convoluted with the AFM tip. Few of the spheres at the surface are in contact with other spheres. When these experiments were repeated on films prepared from samples in which the SDS was removed by ion exchange, the images obtained were identical to the one shown in Figure 7. We thus conclude that even in the presence of SDS surfactant, most of the PBMA spheres are well dispersed in the PEHMA matrix, and the blend morphology is of the type described in the cartoon in Figure 1.

Energy Transfer Experiments. In Table 2 we present the experimental values of the energy transfer efficiencies Φ_{ET} for the PBMA/PEHMA binary blends we examined. For a wide variety of films, the energy transfer efficiency is approximately $\Phi_{ET} = 0.3$, with a small variation between film samples prepared in the presence or absence of SDS surfactant. The difference in energy transfer efficiencies between films annealed at different temperatures is also small.

To fit the experimental fluorescence decay profiles obtained for the PBMA−PEHMA blends to the simulated decays, the noise-free donor decay profiles $I_D(t)$ obtained using eqs 1 and 11 were modified to introduce the features characteristic of real experiments. The simulated donor fluorescence decay profiles were convoluted with the experimental instrument response functions $L(t)$, obtained from the excitation source, as described previously.[31] We refer to the simulated decays convoluted with real lamp excitation profiles as $I_D^{conv}(t)$.

$$I_D^{conv}(t) = \int_0^t L(s)\, I_D(t-s)\, ds \qquad (12)$$

The experimental decay profiles $I_D^{exp}(t)$ profiles were fitted to each of the $I_D^{conv}(t)$ curves, using a linear convolution algorithm. The fitting equation is

$$I_D^{exp}(t) = a_N I_D^{conv}(t) + a_L L(t) \qquad (13)$$

where the fitting parameters are the normalization factor of the decay intensity a_N and the light scattering correction a_L. To evaluate the quality of the fitting results, we calculated the reduced χ^2, the weighted residuals, and the autocorrelation of residuals.

The decay obtained for a blend of PBMA and PEHMA containing 2 wt % of SDS after annealing for 1 h at 60 °C is shown in Figure 8, fitted with a simulated curve corresponding to an interface thickness of $\delta = 23$ nm. We obtain well-distributed autocorrelation plots of the weighted residuals for interface widths from $\delta = 21$ nm to $\delta = 25$ nm, with the best fit at $\delta = 23$ nm. For $\delta = 20$ nm and $\delta = 26$ nm noticeable deviation are apparent, indicating that the profiles simulated for these thicknesses do not fit the experimental decay. We define the error bar for the interface width from the interval of interface width values for which the autocorrelation of the residuals is randomly distributed. In the present case, we obtained acceptable fits for $\delta = 21$ nm to $\delta = 25$ nm, and therefore we consider $\delta = 23 \pm 2$ nm.

For all the experimental decays analyzed, the decay-intensity-normalization and the light-scattering-correction parameters, a_N and a_L, do not change significantly with the variation in the interface thickness value δ. Plots of the reduced χ^2 versus the interface thickness δ (Figures 9 and 10) allow us to compare the results obtained for different films. The values of δ corresponding to the minimum of the χ^2 surfaces are summarized in Table 3. Using the procedure described above (Figure 8), we obtain the optimum values of the interface thickness and the respective error bars for each decay.

Magnitude of the Interface Thickness. In films prepared from latex samples that were purified using an ion-exchange resin, the interface between the PBMA particles and the PEHMA matrix was found to be $\delta = 21 \pm 2$ nm (Figure 9). After annealing 1 h at 60 °C the interface thickness increased to $\delta = 25 \pm 2$ nm. The fact that the interface is already quite broad before annealing is probably related to the low T_g of both components, particularly the PEHMA. A significant amount of polymer segment diffusion must occur during film preparation. After annealing the film above the T_g of PBMA, further interpenetration occurs, and the system appears to reach its equilibrium state.

For the films prepared from unpurified latex dispersions (Figure 10), the results are similar. We find an optimum value of $\delta = 22 \pm 2$ nm in the freshly prepared film. The effect of annealing is less pronounced in this case. After annealing 1 h at 60 °C, the interface thickness increases only slightly to $\delta = 23 \pm 2$ nm. When another film was annealed at 90 °C, also for 1 h, the interface thickness was found to be $\delta = 24 \pm 2$ nm. The major effect of treating the dispersion with an ion-exchange resin is to remove the ionic surfactant SDS and other inorganic salts from the solution. This treatment will also remove oligomeric material produced in the emulsion polymerization if these substances are water-soluble and contain an ionic end group (i.e., $-OSO_3^-$). We conclude that when SDS is present, there

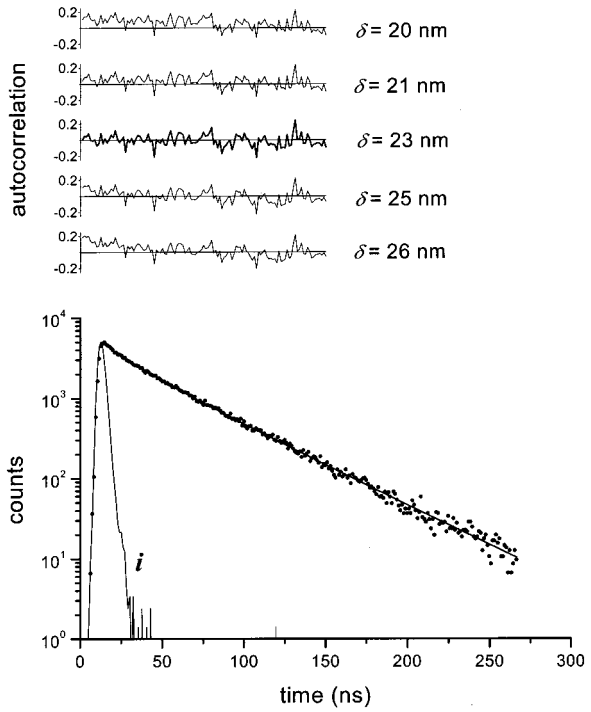

Figure 8. Experimental instrument response function (i) and experimental donor decay profile (●) obtained for a film of a blend of 90 wt % PEHMA and 10 wt % PBMA, annealed for 1 h at 60 °C, fitted to a decay simulated with $\delta = 23$ nm (—). The autocorrelation function plots for the fitting of the curves simulated with interface thicknesses of $\delta = 21$ nm to $\delta = 25$ nm are well distributed, but for $\delta = 20$ nm and $\delta = 26$ nm some deviations are observed.

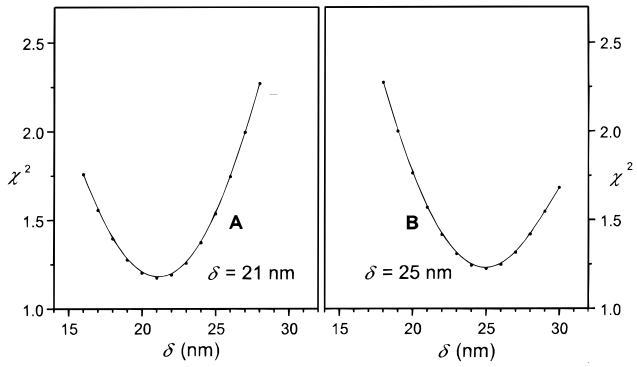

Figure 9. Reduced χ^2 plots from the fit of experimental fluorescence decay profiles obtained for films of a blend of 90 wt % PEHMA and 10 wt % PBMA, cast from a dispersion purified by ion exchange: before annealing (A) and after 1 h at 60 °C (B).

is only a minor effect of annealing upon the interface thickness. Although the effect on the δ values is small, the difference is large enough to be just outside of experimental error (Figure 10).

It is difficult to find a unique explanation for this relatively small effect. The amount of surfactant present (2 wt %) is less than monolayer coverage of the original latex particles. In this type of film, SDS tends to separate into occlusions during film formation. We know from the work of Odrobina[32] that SDS is immiscible with both polymers in the blend and does not act as a plasticizer for either component. The most likely explanation is that ion exchange removes small amounts of oligomeric material that acts to plasticize the surface regions of the PBMA particles. Odrobina and Feng[33] have shown, for example, that one can isolate water-soluble oligomers from the emulsion polymerization of butyl methacrylate. When this material is added to an ion-exchanged PBMA dispersion and films are formed, the additive acts as a plasticizer to promote the rate of polymer diffusion.

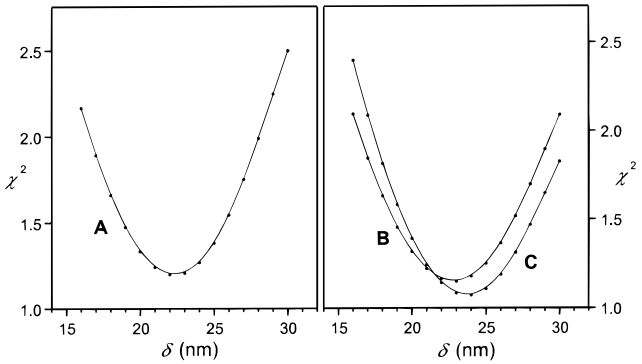

Figure 10. Reduced χ^2 plots from the fit of experimental fluorescence decay profiles obtained for films of a blend of 90 wt % PEHMA and 10 wt % PBMA, containing 2 wt % of SDS surfactant, before annealing (A), after 1 h at 60 °C (B), and after 1 h at 100 °C (C).

Table 3. Average Values of the Interface Thickness δ (nm) in PBMA/PEHMA Binary Blends

	δ (nm)	
	unpurified	ion-exchanged
newly formed film (4 °C)	23 ± 2	
newly formed film (20 °C)	22 ± 2	21 ± 2
annealed 1 h at 60 °C	23 ± 2	25 ± 2
annealed 1 h at 90 °C	24 ± 2	

In the results described above, we found an interface thickness on the order of 20 nm even for freshly prepared latex films. One can sometimes learn about the early stages of film formation by preparing a film at lower temperatures, closer to the minimum film-forming temperature of the major component in the latex blend. We carried out a set of experiments in which the film was prepared from a non-ion-exchanged dispersion cast onto a mica substrate in the cold room, maintained at 4 °C. Water evaporation was slow, and film formation took 3 days. The film was kept cold while it was transferred to a cooled sample holder on the fluorescence decay apparatus. Even for this sample we obtained a value of the interface width $\delta = 23 \pm 2$ nm, which is very similar to what we obtained for the film formed at room temperature. Figure 11 shows a plot of χ^2 against interface width δ for fits to this decay curve, displaying a minimum around 23 nm. Here we do not find evidence for a decrease in the thickness of the interface in films prepared at lower temperature. It is possible that PEHMA is still quite mobile at this temperature, which is higher than its T_g by 15 °C. During the long time that it takes for the film to dry at 4 °C (72 h), some interdiffusion of the polymers can occur.

Overall, we can conclude that the effect of sample preparation on the mixing between the blend components is quite small (Table 3). For blend films containing SDS, we find an average interface thickness of $\delta = 23 \pm 3$ nm, irrespective of annealing history. For the blend film prepared from the ion-exchanged dispersion, we find similar values of the interface thickness and a small increase in this thickness, from $\delta = 21 \pm 2$ nm to $\delta = 25 \pm 2$ nm upon annealing at temperatures above the T_g of the PBMA component. In Figure 12 we plot the calculated donor distribution functions for $\delta = 21$ nm

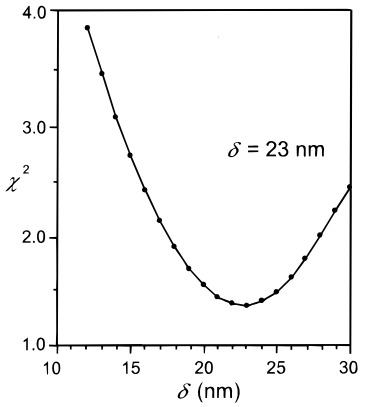

Figure 11. Reduced χ^2 plot from the fit of experimental fluorescence decay profiles obtained for film of a blend of 90 wt % PEHMA and 10 wt % PBMA containing 2 wt % of SDS surfactant. The film was formed at 4 °C, and the fluorescence decay measurements were carried out at the same temperature.

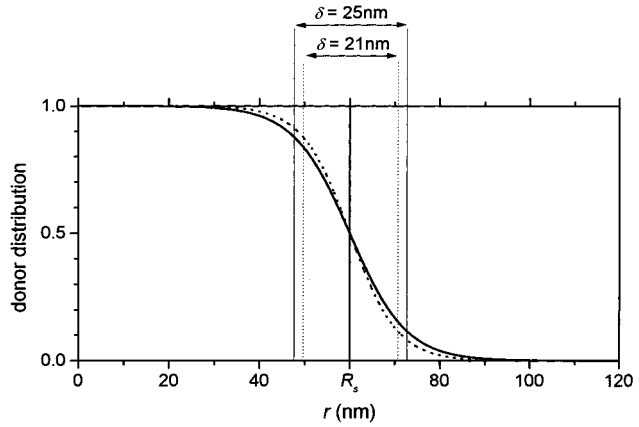

Figure 12. Donor distribution functions calculated for particles with a radius $R_s = 60$ nm and interface thickness, as obtained, and after annealing. The system corresponds to the ion-exchanged (i.e., surfactant-free) blend of 90 wt % PEHMA and 10 wt % PBMA. The overall growth in interface thickness upon annealing, from $\delta = 21$ nm to $\delta = 25$ nm, corresponds to a difference of only 3% in the particle radius $R_s + \delta/2$ but almost 10% in particle volume.

and $\delta = 25$ nm. The overall change in interface thickness from $\delta = 21$ nm to $\delta = 25$ nm upon annealing corresponds to a difference of only 3% in the particle radius, calculated as $R_s + \delta/2$, although it amounts to almost 10% in terms of particle volume. The insensitivity of these blends to annealing is probably related to the low T_g of the blend components and their large molecular weight polydispersity. For the PBMA component, its molecular weight is sufficiently low that its T_g (21 °C by DSC) is decreased by nearly 10 °C over that of higher molecular weight polymer (31 °C by DSC). We imagine that the breadth of the interface is influenced by the low molar mass component of the PBMA, which can most rapidly diffuse and mix with the PEHMA matrix until an equilibrium amount of mixing is attained.

Interface Thickness and the Flory−Huggins Parameter χ. From eq 2 we note that δ depends on the Flory−Huggins χ parameter and the statistical segment length b. If the value of b were known, one could in principle use "measured" values of δ to estimate values of χ. Here we will assume that the average statistical monomer length for PBMA and PEHMA is the same as that of PBMA, $b = 0.6$ nm.[34] Equation 2 applies only to polymers of infinite molecular weight. When the polymer molecular weights are not very high, as in the present case, chain end effects lead to broadening of the interface. As the molecular weight of the polymer decreases, the proportion of the chain ends goes up, increasing the importance of chain end effects. A number of expressions have been proposed by different groups to account for the effect of finite chain length on the relationship between χ and δ in binary polymer blends. These expressions have a similar form but differ in the value assigned to the prefactor K_1: For two polymers of length N_1 and N_2, the interface width is given by the expression:

$$\delta = \frac{2b}{\left[6\left(\chi - K_1\left(\frac{1}{N_1} + \frac{1}{N_2}\right)\right)\right]^{1/2}} \tag{14}$$

We can calculate the value of the χ parameter by rewriting eq 14 as

$$\chi = \frac{2}{3}\frac{b^2}{\delta^2} + K_1\left(\frac{1}{N_1} + \frac{1}{N_2}\right) \tag{15}$$

Broseta et al.[35] find $K_1 = 2 \ln 2$ (=1.386), whereas Stamm et al.[36] report that K_1 is equal to $\pi^2/6$ (=1.645). Stamm et al.[36] point out that the Broseta equation is valid only in the vicinity of the volume fraction $\phi = 0.5$. Considering the experimental errors involved in the determination of δ, both expressions should give equally reliable results for the calculation of χ. Equation 14 was derived for a mixture of two monodisperse polymers. Broseta et al.[35] have shown that the same equations can be used in polydisperse systems if one uses the number-average molecular weight.

The most significant problem in trying to calculate χ values from experimental values of δ is that there are two terms in eq 15. Even for polymers of a relatively high molecular weight, the second term makes a substantial contribution to χ. For our sample of PBMA, $N_n^{PBMA} = 120$. For PEHMA, $N_n^{PEHMA} = 136$. For these samples, the second term is significantly larger than the term containing δ. The unfortunate feature of this result is that the χ parameter is not very sensitive to the value of δ. Taking $K_1 = \pi^2/6$ and an average interface width of 23 nm, we calculate $\chi = 0.026$. This value of χ we calculate is comparable to that reported for blends of polystyrene with PMMA (ca. 0.037), for which the interface is much narrower ($\delta \approx 3-4$ nm).[7] To the extent to which we can have confidence in the magnitude of χ, we infer that our blends correspond to a χN value of about 3, well outside the range expected for strong segregation. To draw a firm conclusion about the strength of the segregation in PBMA-PEHMA blends, we need an independent measure of χ, or we need to repeat these experiments on samples with much higher degrees of polymerization.

Summary

We examined blends of two methacrylate polymers, in which the minor component, PBMA, is present as spheres of uniform size dispersed in a continuous PEHMA matrix. The PBMA was labeled with phenanthrene (Phe) groups; the PEHMA was labeled with anthracene (An) groups. Phe/An represents a useful donor/acceptor pair for direct nonradiative energy transfer (ET) experiments. The blends were prepared by

mixing aqueous dispersions of the polymers in the form of latex nanospheres, casting a film, and allowing the water to evaporate. Upon drying, the soft PEHMA particles ($T_g \approx -10$ °C) in the blend deform and pack to form a continuous matrix. By choosing a ratio of 14 PEHMA particles (diameter 100 nm) per PBMA particle (diameter 120 nm), we ensure that each donor-labeled PBMA droplet in the blend is surrounded by the acceptor-labeled matrix. AFM images of the surface of the film indicate the presence of isolated spheres of 120 nm diameter in a soft PEHMA matrix.

We carried out ET experiments and developed a model to describe energy transfer between donors and acceptors chemically attached to the two different components of a polymer blend. The model describes the case of one polymer dispersed as spheres of identical diameter in a continuous matrix of the second polymer. The model takes explicit account of the segment distribution of the two polymers in the interface region in terms of a modified Helfand−Tagami equation.

We used this model to characterize the interface between the PBMA and PEHMA domains in the blend. In this way we found values of the interface thickness to be $\delta = 22 \pm 2$ nm, a value that hardly changed when the samples were annealed at temperatures above the T_g of PBMA.

In this way we demonstrate that ET experiments provide a useful and powerful method to determine the thickness of the interface between adjacent polymer phases in a polymer blend. The method is applicable to any system in which the dispersed phase can be prepared in the form of uniforms spheres. One of the strengths of the method is that the equations describing the distribution of segments are rigorous for spherical geometries and makes no assumptions about whether the center of the dispersed droplet remains as a "pure phase". For example, in the system examined here, we deduce that there is an interface 22 nm thick at the edge of a droplet whose initial radius was 60 nm. According to the model used to fit the data, one can find small amounts of PEHMA at a distance 2δ inside the edge of the original PBMA droplet. Thus, only the very center of the PBMA droplet is pure PBMA.

A more serious problem is that the model we employed assumed a distribution of polymer segments across the interface described by the theory of Helfand and Tagami. This theory applies to the case of strong segregation. We attempted to calculate a χ value for PBMA−PMMA from the value of $\delta = 22$ nm. Unfortunately, the rather small values of the number-averaged degree of polymerization (N) of our polymers make that calculation difficult. With the best estimate of χ (approximately equal to 0.02−0.03), our blend is characterized by $\chi N \approx 3$, well outside the value appropriate for strong segregation.

In the following paper,[17] we apply this methodology to the study of PEHMA blends with PEHMA copolymers. We find that the presence of carboxylic acid groups in the PEHMA backbone limits the miscibility of these copolymers with PEHMA itself. In those systems, we are able to detect very narrow interfaces in the newly formed latex blends and follow the evolution of the interface thickness as the blends are annealed.

Acknowledgment. The authors thank NSERC Canada for their support of this research. J. P. S. Farinha acknowledges the support of FCT-PRAXIS XXI (Portugal) for his stay in Toronto.

References and Notes

(1) *Polymer Blends*; Paul, D. R., Newman, S., Eds.; Academic Press: New York, 1978.
(2) For a list of miscible polymer blends, see: Krause, S.; Goh, S. H. In *Polymer Handbook*, 4th ed.; Brandrup, J., Immergut, E. H., Grulke, E. A., Eds.; Wiley-Interscience: New York, 1999; pp VI 409−482.
(3) (a) Morawetz, H.; Amrani, F. *Macromolecules* **1978**, *11*, 281. (b) Morawetz, H. *Science* **1979**, *203*, 405. (c) Morawetz, H. *Science* **1988**, *240*, 172. (d) Morawetz, H. *J. Polym. Sci., Part A: Polym. Chem.* **1999**, *37*, 1725.
(4) Helfand, E.; Tagami, Y. *J. Chem. Phys.* **1972**, *56*, 3592.
(5) (a) Ermoshkin, A. V.; Semenov, A. N. *Macromolecules* **1996**, *29*, 6294. (b) Semenov, A. N. *Macromolecules* **1994**, *27*, 2732. (c) Leibler, L. *Macromolecules* **1980**, *13*, 1602.
(6) (a) Zhou, X. L.; Chen, S. H. *Phys. Rep.* **1995**, *257*, 223. (b) Bucknall, D. G.; Butler, S. A.; Higgins, J. S. *J. Phys. Chem. Solids* **1999**, *60*, 1273. (c) Geoghegan, M.; Jones, R. A. L.; Sivia, D. S.; Penfold, J.; Clough, A. S. *Phys. Rev. E* **1996**, *53*, 825, Part B.
(7) Sferrazza, M.; Xiao, C.; Jones, R. A. L.; Bucknall, D. G.; Webster, J.; Penfold, J. *Phys. Rev. Lett.* **1997**, *78*, 3693.
(8) Tan, S. S.; Zhang, D. H.; Zhou, E. L. *Polymer* **1997**, *38*, 4571. (b) Wlochowicz, A.; Janicki, J.; Slusarczyk, C. *Compos. Interface* **1997**, *5*, 1. (c) Foster, M. D. *Crit. Rev. Anal. Chem.* **1993**, *24*, 179.
(9) Birks, J. B. *Photophysics of Aromatic Molecules*; Wiley: London, 1970; Chapter 11.
(10) (a) Cameron, G. G.; Stewart, D.; Buscall, R.; Nemcek, J. *Polymer* **1994**, *35*, 3384. (b) Cameron, G. G.; Quereshi, M. Y.; Stewart, D.; Buscall, R.; Nemcek, J. *Polymer* **1995**, *36*, 3071. (c) Cameron, G. G.; Stewart, D. *Polymer* **1996**, *37*, 5329.
(11) (a) Weber, T. A.; Helfand, E. *J. Chem. Phys.* **1980**, *72*, 4017. (b) Helfand, E. In *Polymer Compatibility and Incompatibility*; Solc, K., Ed.; Harwood: Chur, 1982; p 182.
(12) (a) Winnik, M. A. *Curr. Opin. Colloid Interface Sci.* **1997**, *2*, 192. (b) Keddie, J. L. *Mater. Sci. Eng.* **1997**, *21*, 101.
(13) Farinha, J. P. S.; Martinho, J. M. G.; Kawaguchi, S.; Yekta, A.; Winnik, M. A. *J. Phys. Chem.* **1996**, *100*, 12552.
(14) Yekta, A.; Winnik, M. A.; Farinha, J. P. S.; Martinho, J. M. G. *J. Phys. Chem. A* **1997**, *101*, 1787.
(15) Farinha, J. P. S.; Martinho, J. M. G. *J. Lumin.* **1997**, *72*, 914.
(16) Farinha, J. P. S.; Schillèn, K.; Winnik, M. A. *J. Phys. Chem. B* **1999**, *103*, 2487.
(17) Pham, H.; Farinha, J. P. S.; Winnik, M. A. *Macromolecules* **2000**, *33*, 5850.
(18) Feng, J.; Winnik, M. A. *Macromolecules* **1997**, *30*, 4324.
(19) Phillips, D.; O'Connor, D. V. *Time Correlated Single Photon Counting*; Academic Press: London, 1984.
(20) James, D. R.; Demmer, D. R. M.; Verral, R. E.; Steer, R. P. *Rev. Sci. Instrum.* **1983**, *54*, 1121.
(21) Martinho, J. M. G.; Egan, L. S.; Winnik, M. A. *J. Anal. Chem.* **1987**, *59*, 861.
(22) Förster, Th. *Ann. Phys. (Leipzig)* **1948**, *2*, 55.
(23) Förster, Th. *Z. Naturforsch.* **1949**, *4A*, 321.
(24) Wang, Y.; Zhao, C. L.; Winnik, M. A. *J. Chem. Phys.* **1991**, *95*, 2143.
(25) Baumann, J.; Fayer, M. D. *J. Chem. Phys.* **1986**, *85*, 4087.
(26) Although PEHMA has a T_g below room temperature, we assume that the dipoles are randomly oriented and frozen on the nanosecond time scale of the energy transfer experiment. In this case we can use the value $\kappa^2 = 0.478$.[25]
(27) Martinho, J. M. G.; Farinha, J. P. S.; Berberan-Santos, M. N.; Duhamel, J.; Winnik, M. A. *J. Chem. Phys.* **1992**, *96*, 8143.
(28) Lyness, J. N. *SIAM Rev.* **1983**, *25*, 63.
(29) Feng, J.; Pham, H.; Stoeva, V.; Winnik, M. A. *J. Polym. Sci., Part B: Polym. Phys.* **1998**, *36*, 1129.
(30) (a) Vorobyova, O. Ph.D. Thesis, University of Toronto, 2000. (b) Vorobyova, O.; Winnik, M. A. *Macromolecules*, submitted for publication.
(31) Farinha, J. P. S.; Martinho, J. M. G.; Pogliani, L. *J. Math. Chem.* **1997**, *21*, 131.
(32) Odrobina, E. Ph.D. Thesis. University of Toronto, 2000.
(33) Odrobina, E.; Feng, J.; Winnik, M. A. *J. Polym. Sci., Part A: Polym. Chem.*, in press.
(34) Helfand, E.; Sapse, A. M. *J. Chem. Phys.* **1975**, *62*, 1327.
(35) Broseta, D.; Fredrickson, G. H.; Helfand, E.; Leibler, L. *Macromolecules* **1990**, *23*, 132.
(36) Stamm, M.; Schubert, D. W. *Annu. Rev. Mater. Sci.* **1995**, *25*, 325.

MA0000935